CONTROL DEWAR VENTURI CALIBRATION EXPLANATION FOR TOSHIBA

D0 Engineering Note: 3823.000-EN-462
January 24, 1997

Andrew Kuwazaki
PPD-ETT D0 Upgrade Group

Approved By

ID #8351

This document is intended to explain the calibration data for the venturi, FE-3253-H, which is installed in the control dewar. Further, this document will help explain how to use the venturi to make mass flow measurements during typical operating conditions. The purpose of the calibration data enclosed from the Colorado Engineering Experiment Station Inc. is to experimentally show that the venturi follows the flow equation below which is also enclosed as Eq. 7-36 on page 155, from the Applied Fluid Dynamics Handbook:

$$\dot{m} = C\frac{\pi d^2}{4}\left[\frac{1}{1-\left(d/D\right)^4}\right]^{\frac{1}{2}}\left[2\rho_1\left(p_1 - p_2\right)\right]^{\frac{1}{2}} Y .$$

The calibration data serves to show that the Subsonic Venturi, Serial Number 611980-18, produces results predicted by the compressible subsonic flow mass flow rate equation above and to experimentally determine the discharge coefficient C. Colorado Engineering Experiment Station Inc. ran tests at 15 independent differential pressures to conclude that use of this venturi will perform according to the mass flow rate equation above.

In order to verify the results from the Colorado Engineering Experiment Station Inc. we have provided you with a step-by-step procedure using the values they have chosen.

The values chosen correspond to L = 1 on the Colorado Engineering Experiment Station Inc. data sheet. Using Eq. 7-36 we will calculate the mass flow rate. The coefficient of discharge, C or Cd, for a machined venturi is nominally 0.995 as seen in Table 7-7, number 2. The throat diameter, d, is 0.136 inches and the inlet diameter, D, is 0.5 inches. The density is given as 10.11 pound mass per cubic foot. And the measured pressure differential is 932.490 psid. Plugging these values into Eq. 7-36 gives:

$$\dot{m} = .995\frac{\pi(.136in.)^2}{4}\left[\frac{1}{1-(.136in./.5in.)^4}\right]^{\frac{1}{2}}\left[2\left(10.11\frac{lbm}{ft^3}\right)\left(932.49\frac{lb}{in.^2}\right)\right]^{\frac{1}{2}} Y. \quad [1]$$

We will use g_c to relate the force, lb, and the mass, lbm together. Then we can arrive at the proper units of pound mass per second (lbm/s) for the mass flow rate.

$$g_c = 32.2\frac{lbm - ft/s^2}{lb}. \qquad [2]$$

We will also convert feet to inches.

Therefore, the mass flow rate is:

$$\dot{m} = \left(.94111\frac{lbm}{s}\right)Y \qquad [3]$$

In order to finish solving for the mass flow rate, we must determine the Expansion Factor Y. Y can be calculated from Eq. 7-29 which is provided in the following pages or for gases with a specific heat ratio of 1.4, Table 7-3, Expansion Coefficients for Nozzles, page 137 in Applied Fluid Dynamics Handbook can be used. We need three pieces of information to use Table 7-3. First notice that the ratio of the specific heats for air is 1.4 as given by the Colorado Engineering Experiment Station Inc. Therefore, we will use the bottom half of Table 7-3 corresponding to an Expansion Factor Y for the ratio 1.4. Secondly, the ratio of the throat diameter to the inlet diameter(d/D) is:

$$d/D = (.136/.5) = .272. \qquad [4]$$

Since the actual ratio, .272 is closest to the given ratio .3 on the left-hand column of Table 7-3, we will use the ratio .3. Thirdly, the Pressure Ratio is the ratio of the static pressure at the nozzle throat to the static pressure upstream of the nozzle and is calculated as follows:

$$\frac{p_2}{p_1} = \frac{(2002.4 - 932.4)}{2002.4} = \frac{1070}{2002.4} = .534 \qquad [5]$$

Since the actual ratio of .534 is closest to the given ratio of .55 in Table 7-3, we will use .55. Knowing these values we can read off Table 7-3 the appropriate Expansion Factor, Y=.7193.

Now that we have chosen the correct Expansion Factor we can continue to solve for the mass flow rate. Using Eq. 3 above, the mass flow rate(lbm/sec) becomes,

$$\dot{m} = \left(.94111\frac{lbm}{s}\right)Y = \left(.94111\frac{lbm}{s}\right)(.7193) = 6.769E-001. \qquad [6]$$

The value given by the Colorado Engineering Experiment Station Inc. for the same conditions above is 6.9090E-001 pound mass per second. Differences in the calculated value to the actual value can be compensated by adjusting the value of the discharge coefficient C. C is defined as the ratio of the actual flow rate to the measured flow rate. In our case C was found to be (6.909/6.769)=1.02, which is more or less the value listed in the discharge coefficient column provided by the calibration data.

We will now go through an example using the properties of Helium which are similar to those expected during operating conditions. Once again we will use Eq. 7-36. These calculations will be done in SI units.

First we will state the given information. The coefficient of discharge, C, will be approximately 1. The throat diameter in meters is 3.4544E-3 (.136 inches). The inlet diameter is 1.27E-2 m (.5 inches). In order to determine the density of helium will use the Thermophysical Properties of Helium which is also enclosed. A typical operating pressure will be 0.120 MPa. The helium will typically be subcooled to a temperature of about 4.3 Kelvin. Since 4.3 K does not have its own entry we must interpolate between the temperatures 4.2 and 4.407 Kelvin. Upon interpolating, the density at 4.3 Kelvin is 123.9 kilograms per cubic meter.

At the typical conditions during a flow test, the pressure differential is approximately 0.43 inches of water. The conversation factor from English to SI units is 1 in. of water equals 248.8 Newton per square meter. A Newton per square meter is also known as a Pascal. Therefore, the differential pressure in SI units is:

$$dp = .43 \text{ in. } H_2O\left(\frac{248.8 \text{ N/m}^2}{1 \text{ in. } H_2O}\right) = 106.984 \ \frac{\text{N}}{\text{m}^2} \qquad [7]$$

Now we can insert values into the variable in Eq. 7-36.

$$\dot{m} = 1.00\frac{\pi(3.4544E-3)^2}{4}\left[\frac{1}{1-(3.4544E-3/1.27E-2)^4}\right]^{\frac{1}{2}}\left[2\left(123.9\frac{kg}{m^3}\right)\left(106.984\frac{N}{m^2}\right)\right]^{\frac{1}{2}}Y$$

Equation 8

Noting in Eq. 8 that a Newton is equal to a kilogram-meter per square second, we can simplify the equation above to:

$$\dot{m} = \left(1.530E-3\ \frac{\text{kg}}{\text{s}}\right)Y = \left(1.530\ \frac{\text{g}}{\text{s}}\right)Y \qquad [9]$$

The mass flow rate is not complete until we determine the Expansion Factor Y. However, unlike the previous example, we must calculate Y with Eq. 7-29 on page 136 in the Applied Fluid Dynamics Handbook.

$$Y = \left[r^{2/\gamma}\left(\frac{\gamma}{\gamma-1}\right)\left(\frac{1-r^{(\gamma-1)/\gamma}}{1-r}\right)\frac{1-(d_2/d_1)^4}{1-(d_2/d_1)^4 r^{2/\gamma}}\right]^{\frac{1}{2}}$$

In order to solve for the Expansion Factor Y, we must know the ratio of the throat static pressure to the inlet static pressure. This ratio is noted as 'r'. If the inlet static pressure is 0.12 MPa and the pressure differential is 1.070E-4 MPa, as calculated in Eq. 7, then the throat static pressure must be 0.1199 MPa. Therefore the ratio is as follows:

$$r = \frac{p_2}{p_1} = \frac{.1199}{.120} = .999 \qquad [10]$$

We must now refer back to the Thermophysical Properties Table for Helium to determine the ratio of the specific heats. Interpolating once again for a temperature of 4.3 Kelvin, the specific heat at constant pressure is 5.523 Joules per gram-Kelvin, and the specific heat at constant pressure is 2.157 Joules per gram-Kelvin. And the ratio is:

$$\gamma = \frac{5.523\frac{J}{g-K}}{2.560\frac{J}{g-K}} = 2.157 \qquad [11]$$

Now using Eq. 7-29 above, we can solve for the Expansion Factor:

$$Y = \left[.999^{2/2.157}\left(\frac{2.157}{2.157-1}\right)\left(\frac{1-.999^{(2.157-1)/2.157}}{1-.999}\right)\frac{1-(3.4544E-3/1.27E-2)^4}{1-(3.4544E-3/1.27E-2)^4(.999)^{2/2.157}}\right]^{\frac{1}{2}}$$

By solving this equation, the Expansion Factor Y=.999 or approximately 1. Therefore, we can continue to solve for the mass flow rate by inserting Y=1 into Eq. 9.

$$\dot{m} = \left(1.530\frac{g}{s}\right)Y = \left(1.530\frac{g}{s}\right)(1) = 1.530\frac{g}{s} \qquad [12]$$

We hope that with these two examples you will better understand the calibration data given by Colorado Engineering Experiment Station Inc. as well as better understand how to obtain measurements from the venturi installed in the control dewar.

Fox Valve Development Corp.
HAMILTON BUSINESS PARK, UNIT 6A FRANKLIN RD.
DOVER, NJ 07801
(201) 328-1011 FAX:(201) 328-3651

FROM TFF-087

2/6/96

Certificate of Hydrotest

C.T. Takahashi & Co. P.O. CTA-5041

Item:	**ΔP Venturi Flowmeter**
Fox Part No.:	**611980-18**
Installation Drawing No.:	**614024**
Customer's Designation:	**FE 3253-H**
Customer's Drawing No.:	**3KN114719**

This certifies that the above referenced venturi flowmeter has been hydrostatically tested to 225 psig. No leakage or deformation was noted.

Tested by [signature]

Test date JAN. 4, 1996

JOB NO. M221136 KE 0020
DWG NO. 3KN114719P001
O/# K177AC100

Robert R. Lee

Applications Engineer

/081-0455001412-(‡997) /96-05-03-18:45/001-024 081-31954-TOSHIBA

DO NOT SCALE DRAWING

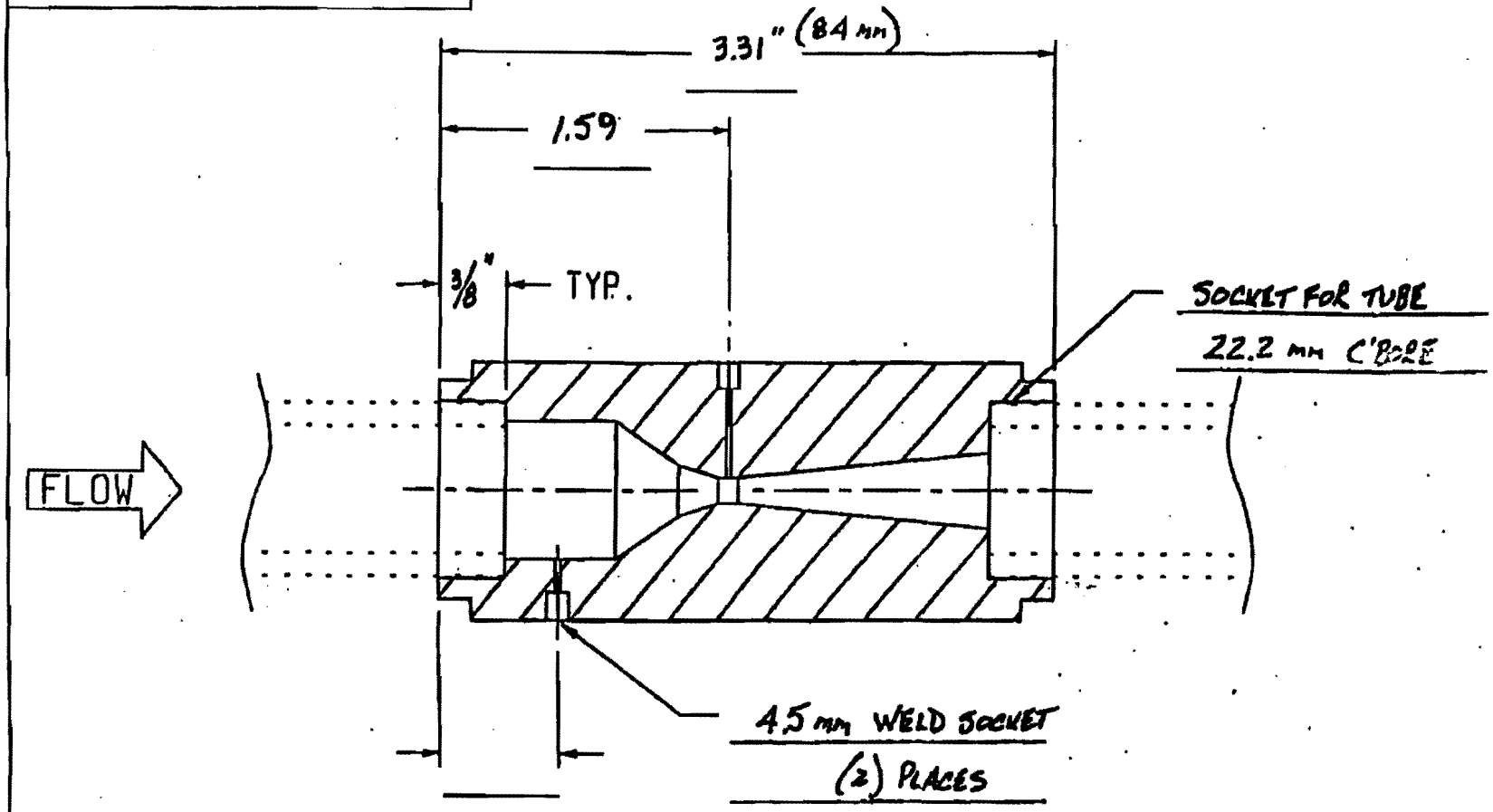

FE-3253-H

Fox Part No. 611980-18
Material 304 L SS
Line Size 7/8" OD TUBE
Design Conditions $\rho = 7.69\ \#/ft^3$
0.011 #/SEC LIQ HE @ ΔP = 0.18 psid
Throat Dia. .136
Customer Info: FERMILAB/TOSHIBA/TAKAHASHI
P.O. CTA-5041

CONTRACT NO		FOX VALVE DEVELOPMENT COR
APPROVALS	DATE	INSTALLATION DRAWING FOR SOCKET WELD ΔP VENTURIES (SOCKET WELD T
DRAWN BY BC	3/16/95	
MATERIAL		SIZE B · REVISION · DRAWING NO 614024
FINISH		SCALE · SHEET OF

/081-0455001412-(#997") /96-05-03-18:45/001-025
1954-TOSHIBA

COLORADO ENGINEERING
EXPERIMENT STATION INC.

CERTIFICATE OF CALIBRATION

This calibration is traceable to the

NATIONAL INSTITUTE OF STANDARDS AND TECHNOLOGY

Serial Number: 611980-18

For: Fox Valve Development Corp. Order: LSF12-19-95A

Data File: 96FXV001 Disc: 0196-039 Date: 29 January 1996

The uncertainty in indicated flowrate is estimated to be +/- 0.5 % of reading to 95% confidence.

The calibration identified by the above CEESI data file was performed using standards that are traceable to the National Institute of Standards and Technology.

This calibration was performed in accordance with the current revision of PROC-10 and MIL-STD 45662A.

This Calibration is: [X] As Found [X] As Left

Calibration performed by:

Quality Assurance

Steve Caldwell
Vice President

Re-calibration is recommended to be no more than 12 months from the date of this Certificate

JOB NO. M221136 KE 0020
DWG NO. 3KN114719P001
O/# K177AC100

/081-0455001412=(*777) /96-05-03-18:45/001-026
081-31954=TOSHIBA

LABORATORY/OFFICE:
54043 County Rd. 37
Munn. Colo. 80648
Phone: 970-897-2711
FAX: 970-897-2710

COLORADO ENGINEERING EXPERIMENT STATION INC.

Calibration of a Subsonic Venturi
Serial Number: 611980-18
For: Fox Valve Development Corp. Order: LSF12-19-95A
Data File: 96FXV001 Disc: 0196-039 Date: 29 January 1996
Inlet diameter: .5 inches Throat diameter: .136 inches
Test gas: AIR Standard density= .074915 lbm/cu-ft
at standard conditions of 529.69 deg R, and 14.696 psia
Cd: Coefficient of Discharge
Flow: Mass flowrate in pounds per second
Diff: Differential pressure in psid
Rey No: Throat Reynolds number
Press: Inlet static pressure in psia
Temp: Inlet temperature in degrees Rankine
Density: Inlet density in pounds mass per cubic foot
Ratio of specific heats: 1.4

L	Diff	Density	Cd	Rey No	Temp	Press	Flow
1	932.490	10.1100	1.0317	6.308E+006	534.4	2002.400	6.9090E-001
2	506.750	10.1100	1.0070	5.465E+006	534.5	2002.400	5.9870E-001
3	439.340	10.1100	1.0033	5.194E+006	534.5	2002.400	5.6900E-001
4	369.340	10.1000	1.0032	4.876E+006	534.6	2002.400	5.3422E-001
5	437.550	10.1100	1.0032	5.190E+006	534.2	2002.400	5.6833E-001
6	319.720	10.1100	1.0011	4.604E+006	534.4	2002.400	5.0431E-001
7	274.080	10.1000	0.9975	4.308E+006	534.6	2002.400	4.7199E-001
8	211.780	10.1000	1.0006	3.870E+006	534.8	2002.400	4.2414E-001
9	165.550	10.0900	0.9961	3.451E+006	535.1	2002.400	3.7841E-001
10	215.570	10.1000	0.9998	3.896E+006	534.9	2002.400	4.2705E-001
11	188.920	10.1000	0.9989	3.673E+006	534.9	2002.400	4.0264E-001
12	147.980	10.0900	0.9944	3.274E+006	535.1	2002.400	3.5901E-001
13	123.920	10.0900	0.9929	3.010E+006	535.4	2002.400	3.3020E-001
14	101.160	10.0800	0.9877	2.721E+006	535.7	2002.400	2.9863E-001
15	125.020	10.0800	0.9919	3.018E+006	535.6	2002.400	3.3115E-001

Average values for above results:
Press: 2002.4 psia Density: 10.099 lbm/cu-ft
Temp: 534.84 Deg R Viscosity: .0000010261 lbm/inch-sec
Compressibility factor: 1.0007

081-31954-TOSHIBA /081-0455001412=(‡ᵞ77") /96-05-03-18:45/001-027

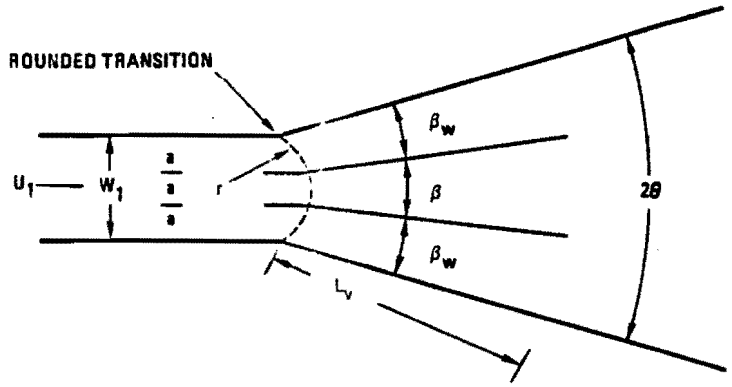

Fig. 7-16. Feil's vane system installed in a two-dimensional diffuser.

θ_* is here measured in radians. $2\theta_*$ is the sum of the diffuser included angle and a correction angle which is dependent only on the diffuser area ratio:

$$2\theta_* = 2\theta + 2\Delta\theta, \tag{7-62}$$

where $\Delta\theta$ in degrees is given below:

A_2/A_1	3.0	3.5	4.0	4.5	5.0
$\Delta\theta$ (deg)	4.5	6.0	6.7	7.3	7.5

The number of vanes is chosen so that

$$\beta = 2\theta_*/(n + 1) \cong 7° \text{ to } 10°,$$

where n is the number of vanes. The spacing between vanes is $a = W_1/(n + 1)$ (Fig. 7-16). The length of the vanes L_v is chosen as either 0.6 times the length of the diffuser side L or such that each diffusing passage operates at the line of appreciable stall as indicated in Fig. 7-7 for a two-dimensional diffuser, whichever is shorter.

While the rules presented in the previous two paragraphs were developed for two-dimensional diffusers, it is reasonable to believe, in the absence of contrary published data, that they can be applied directly to conical and annular diffusers.

Curved Wall Diffusers. Curved wall diffusers can be of two classes: (1) diffusers whose axis is straight but whose walls are curved in a bell or a trumpet shape, or (2) diffusers whose axis is curved so that the diffuser is the sum of a bend and a straight axis diffuser. Tests by Carlson et al. (Ref. 7-28) indicate that there is little advantage in utilizing a trumpet or bell wall shape over a straight wall in a straight axis, two-dimensional diffuser; moreover, the straight wall design is far easier to construct.

The losses in a curved axis diffuser (a diffusing bend) exceed those in a comparable straight axis diffuser. The pressure recovery is lower, and the bending of the flow results in an exit maldistribution with higher flow velocities on the outside of the bend. However, a curved axis diffuser can be more efficient than the combination of a straight axis diffuser and a bend (Ref. 7-48). Considerable data on curved axis diffusers is presented in Refs. 7-29, 7-48, 7-57, and 7-58.

7.6. VENTURI TUBES

Venturi tubes are the union of a nozzle and a diffuser, as shown in Fig. 7-17. The purpose of a venturi tube is to create a region of low static pressure at the venturi throat which can be used to draw in a second fluid, as in a venturi carburetor, or to generate a pressure differential between the throat static pressure and the static pressure in the contiguous pipe line, as in a venturi flowmeter.

The mass flow rate through a venturi tube can be predicted by the same formulas for nozzles that are developed in Section 7.2. For incompressible flow, the mass flow rate is [Eq. (7-33)]

$$\dot{m} = C\,\frac{\pi d^2}{4}\left[\frac{1}{1-(d/D)^4}\right]^{1/2}[2\rho\,(p_1 - p_2)]^{1/2}.$$

For compressible subsonic flow, the mass flow rate is [Eq. 7-36)]

$$\dot{m} = C\,\frac{\pi d^2}{4}\left[\frac{1}{1-(d/D)^4}\right]^{1/2}[2\rho_1(p_1 - p_2)]^{1/2}Y.$$

C is the discharge coefficient, i.e., the ratio of the actual flow rate to the ideal flow rate for a given static pressure differential. p_1 is static pressure at the upstream tap where the diameter is D, and p_2 is the static pressure at the throat where the diameter is d. ρ is density and ρ_1 is the density at the upstream tap (see discussion at end of Section 7.2.3). Y is the expansion coefficient [Eq. (7-29), Table 7-3]. Consistent sets of units are given in Table 3-1.

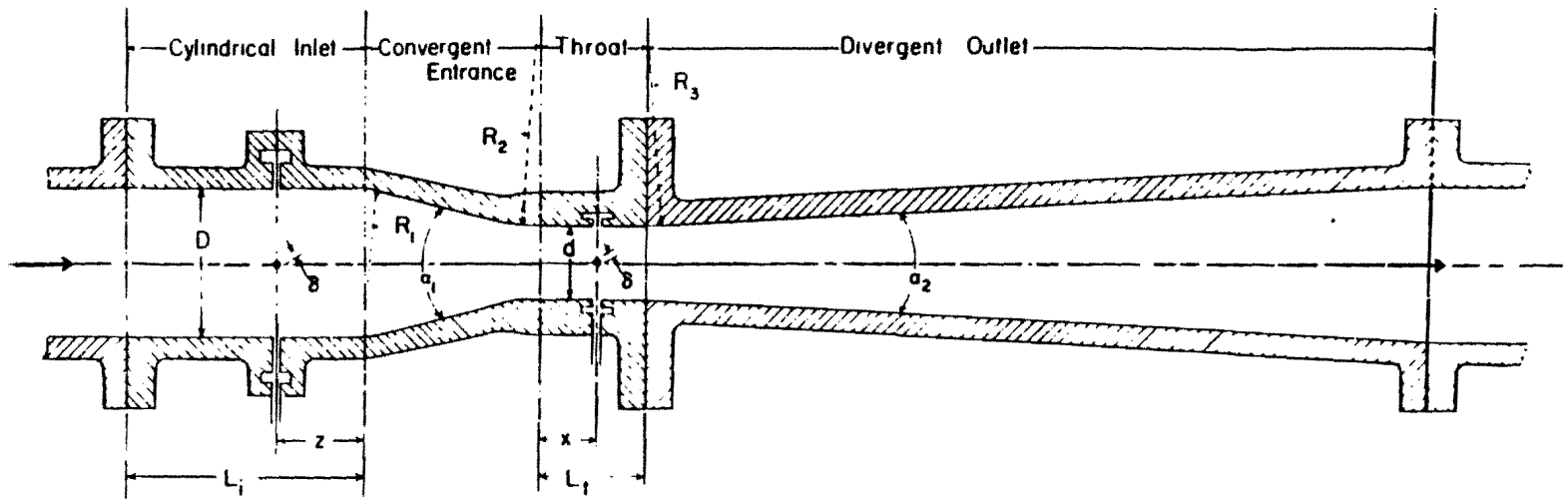

$L_i \gtrless D$ or $L_i \gtrless (D/4 + 10")$
$z \gtrless D/2 \pm D/4$ for $4" \gtrless D \gtrless 6"$
$D/4 \gtrless z \gtrless D/2$ for $6" \gtrless D \gtrless 32"$

$R_1 = 1.375\ D \pm 20\%$
$R_2 = 3.625\ d \pm 0.125\ d$
$5d \gtrless R_3 \gtrless 15d$

$L_t \gtrless d/3$
$y \gtrless d/6$
$5/32" \gtrless \delta \gtrless 25/64"$ and $\delta < 0.1\ D$ or $0.13\ d$
$\alpha_1 = 21° \pm 1°$
$7° \gtrless \alpha_2 \gtrless 8°$ or $7° \gtrless \alpha \gtrless 15°$

(a) ASME Herschel venturi tube. " denotes inch (Ref. 7-10)

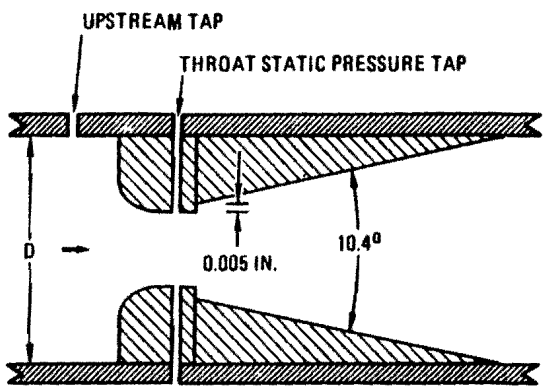

(b) ASME nozzle with attached diffuser (Ref. 7-59, also see Fig. 7-3)

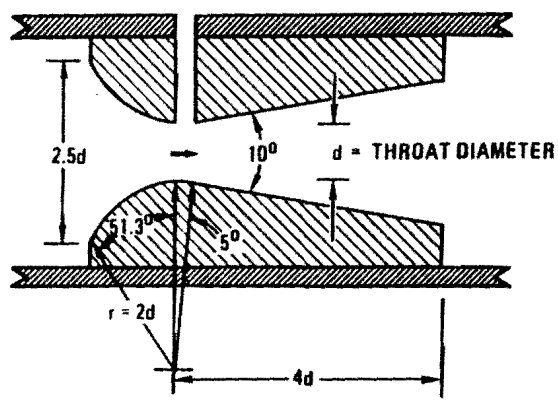

(c) ISA circular arc venturi (Ref. 7-60)

Fig. 7-17. Three venturi tube flowmeter designs.

Since p_2 decreases with decreasing flow area of the venturi throat, the pressure differential $p_1 - p_2$ is maximized by decreasing the throat area. The discharge coefficient C is the ratio of the actual flow through the venturi to the one-dimensional ideal flow rate for a given pressure differential $p_1 - p_2$ (Section 7.3). C is nearly always between 0.995 and 0.985 for most continuous venturi tubes, as shown in Table 7-7. For the ASME modified nozzle venturi, the ASME nozzle discharge coefficients are used [Fig. 7-17(b), Ref. 7-10].

In constructing venturi tubes, considerable precision must be used in machining the throat section so that the resultant flowmeter will conform to the discharge coefficients of Table 7-7. The American Society of Mechanical Engineers (ASME) recommends that the throat section be polished to a mean surface roughness no greater than 5×10^{-6} d, where d is the throat diameter (Ref. 7-10). The static pressure taps should be drilled perpendicular to the nozzle axis with openings into the flow that are sharp and free of burrs. The diameter of the static pressure taps should not exceed approximately 1/10 the throat diameter. Tolerances and installation details for the ASME Herschel venturi tube and other flowmeters are given in Ref. 7-10. ISO recommendations are given in Ref. 7-18.

The principal advantage of the venturi flowmeter over the square-edged orifice plate (Section 6.5.3) or the flow

Table 7-7. Discharge Coefficients for Venturi Tube Flowmeters.
Notation: D = diameter of contiguous pipe; d = throat diameter of venturi; U = average flow velocity through contiguous pipe; U_d = average velocity through throat; ν = kinematic viscosity.
1 inch = 25.4 mm. See Fig. 7-18. (Refs. 7-10, 7-59 through 7-62.)

Venturi Tube	Parameter Range	Discharge Coefficient, C [(a)]
1. ASME Herschel, rough cast entrance cone	$100\ \text{mm} \le D \le 800\ \text{mm}$ $0.3 \le d/D \le 0.75$ $2 \times 10^5 \le UD/\nu \le 2 \times 10^6$	$0.984 \pm 0.7\%$
2. ASME Herschel, machined entrance cone	$50\ \text{mm} \le D \le 250\ \text{mm}$ $0.4 \le d/D \le 0.75$ $2 \times 10^5 \le UD/\nu \le 10^6$	$0.995 \pm 1.0\%$
3. ASME Herschel, rough-welded sheet metal entrance cone	$200\ \text{mm} \le D \le 1200\ \text{mm}$ $0.4 \le d/D \le 0.70$ $2 \times 10^5 \le UD/\nu \le 2 \times 10^6$	$0.985 \pm 1.5\%$
4. ASME flow nozzle with attached 10° diffuser (See Section 7.3.2)	$50\ \text{mm} < D < 400\ \text{mm}$ $0.37 \le d/D \le 0.76$ $10^5 < U_d d/\nu < 5 \times 10^6$	$0.9961 - \dfrac{4.73}{(U_d d/\nu)^{1/2}} \pm 0.7\%$
5. ISA circular arc	$10^5 < U_d d/\nu \le 10^7$	$0.9935 - \dfrac{1.525}{(U_d d/\nu)^{1/2}}$
6. Universal Venturi Tube (U.V.T.)	$4 \times 10^4 < UD/\nu < 2 \times 10^6$	$0.9797 \pm 0.75\%$

(a) Eqs. 7-31, 7-33, 7-36.

nozzle (Section 7.3.2) is that the diffuser section minimizes the total pressure loss. For example, the loss in total pressure for flow through the meter can be expressed as a fraction of the differential static pressure between the inlet and the throat for these ASME meters (Ref. 7-10):

$$\frac{\text{Overall Pressure Loss}}{\text{Differential Pressure}} = \left(\frac{p_1 - p_3}{p_1 - p_2}\right)^a$$

ASME Flowmeter	Throat Diameter/Pipe Diameter, d/D						
	0.2	0.3	0.4	0.5	0.6	0.7	0.8
Square-edged orifice	0.93	0.89	0.82	0.74	0.63	0.53	0.38
Long-radius nozzle	0.95	0.85	0.75	0.65	0.53	0.42	0.29
Venturi tube 15° outlet	0.30	0.25	0.20	0.17	0.13	0.11	0.12
Venturi tube 7° outlet	0.15	0.13	0.12	0.11	0.11	0.11	0.12

[a] p_1 is the upstream static pressure, p_2 is the throat static pressure, and p_3 is the static pressure at a point well downstream.

The superior performance of the venturi tube compensates for its length and higher fabrication costs when used in low-loss systems. The ISO circular arc venturi tube will have a greater overall loss than the ASME venturi tube owing to the sudden expansion four throat diameters downstream of the nozzle throat, as shown in Fig. 7-17(c). The Universal Venturi Tube, shown in Fig. 7-18, has a low loss, comparable to that of the ASME venturi tube with a 7° outlet, and it has the added benefit of being nearly 40% shorter.

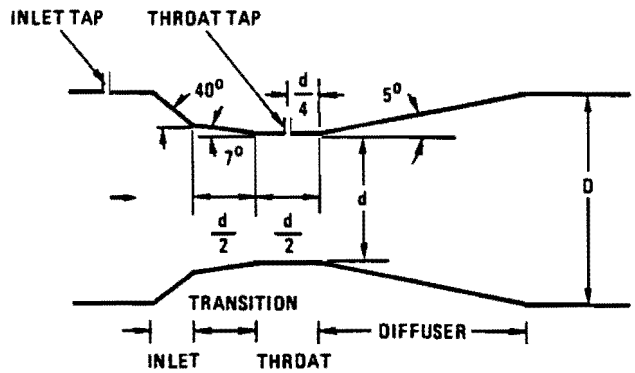

Fig. 7-18. Universal Venturi Tube (Refs. 7-61, 7-62).

7.7. EXAMPLES

7.7.1. Nozzle Example

A test of a water jet propulsion system is shown in Fig. 7-19. A pump discharges through a flexible bellows into a right angle section of pipe, which in turn discharges through a nozzle into a reservoir. The thrust of the jet is measured by a force gauge. In order to optimize the design, it is desired to pick the nozzle opening diameter d which produces the maximum thrust given the following pump characteristics at a constant pump rotation speed:

Discharge pressure above inlet (10^5 Pa)	2.5	2.0	1.5	1.0	0.5
Discharge volume (m^3/sec)	0.12	0.15	0.20	0.22	0.23

This decrease in volume flow with increasing discharge pressure is typical of turbine pumps. The units of frame 1 of Table 3-1 will be used in this example.

The decrease in fluid static pressure between sections 1 and 2 in Fig. 7-20 is due to the frictional losses of the straight pipe section and the bend. Using Chapter 6, Eqs. (6-6) and (6-15), the difference in static pressure between 1 and 2 is

$$p_1 - p_2 = \frac{1}{2}\rho U^2\left[K_{bend} + \frac{f(L_1 + L_2)}{D}\right],$$

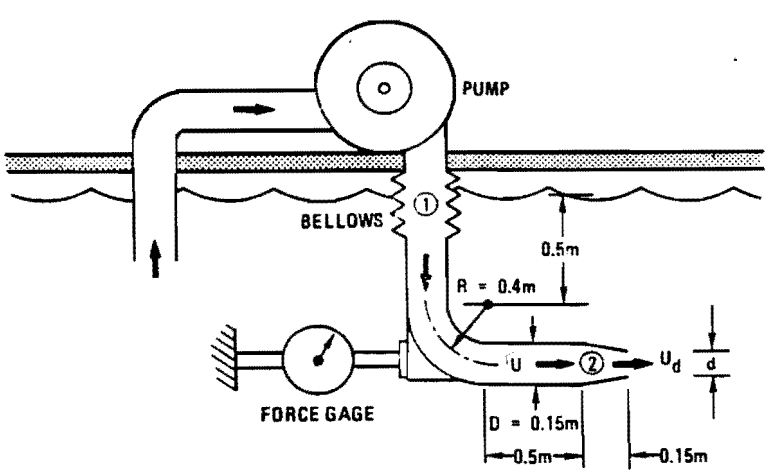

Fig. 7-19. Test of a water jet propulsion system.

4

Equations (7-27) and (7-28) are identical to the corresponding equations for incompressible flow [Eqs. (7-4) and (7-5)] except that the density is referenced to section 1 and the expansion factor Y has been introduced into Eq. (7-28) and the factor $r^{-1/\gamma}Y$ into Eq. (7-27). The expansion factor Y is a function of the static pressure ratio and the ratio of specific heats (Ref. 7-10, p. 52),

$$Y = \left[r^{2/\gamma} \left(\frac{\gamma}{\gamma - 1} \right) \left(\frac{1 - r^{(\gamma-1)/\gamma}}{1 - r} \right) \frac{1 - (A_2/A_1)^2}{1 - (A_2/A_1)^2 r^{2/\gamma}} \right]^{1/2}. \tag{7-29}$$

Values of Y are presented in Table 7-3. If the nozzle areas are circular, which is the most common case, the area ratio $(A_2/A_1)^2$ may be replaced by $(d_2/d_1)^4$, where d_2 and d_1 are the diameters corresponding to the areas A_2 and A_1.

The upstream density ρ_1 must be known to apply Eq. (7-28) in computing the flow rate. ρ_1 can be determined from an overall flow model, but it is more commonly computed using the perfect gas law and the measured static pressure p_1 and the static temperature T_1. Both p_1 and T_1 must be measured. Ordinarily, a thermometer or thermocouple inserted into the upstream flow will measure the stagnation temperature (actually the recovery temperature, which is very nearly the isentropic stagnation temperature) rather than the static temperature. The static temperature will be within 2% of the stagnation temperature for air at Mach numbers less than M = 0.3. For Mach numbers in excess of $M_1 = 0.3$, the static temperature can be computed from a measurement of the stagnation temperature as follows: (1) measure the stagnation temperature at 1, and estimate the flow velocity U_1 and speed of sound c_1; (2) calculate the static temperature at 1 using $M_1 = U_1/c_1$ and Eq. (7-15); (3) compute ρ_1 using the perfect gas law and the measured value of p_1 and the value of T_1 computed in step 2, $\rho_1 = p_1/(RT_1)$; (4) calculate the mass flow rate from Eq. (7-28), the flow velocity $U_1 = \dot{m}/(\rho_1 A_1)$, and the speed of sound $c_1 = (\gamma R T_1)^{1/2}$; and (5) iterate, returning to step 2, until the procedure converges and the desired accuracy is obtained. Ordinarily, only one or two iterations are required.

The maximum flow through a nozzle occurs, as has been shown by Eqs. (7-20) and (7-21), when the velocity in the throat of the nozzle is sonic. If the area of the throat is A_2, the static pressure at the throat is p_2, and the static pressure and flow area at some upstream point are p_1 and A_1, then the following equation relates the flow area ratio to the static pressure ratio which just produces sonic velocity at the throat (Ref. 7-10, p. 68):

$$\left(\frac{p_2}{p_1}\right)^{(1-\gamma)/\gamma} + \frac{\gamma - 1}{2}\left(\frac{A_2}{A_1}\right)^2 \left(\frac{p_2}{p_1}\right)^{2/\gamma} = \frac{\gamma + 1}{2}. \tag{7-30}$$

Solutions for this critical pressure ratio are given in Table 7-4. Pressure ratios p_2/p_1 above the critical pressure ratio yield subsonic flow. Pressure ratios lower than the critical ratio, as obtained for example by lowering the outlet pressure, will establish shock waves in the exit stream from the nozzle throat.

Equation (7-28) will overpredict the mass flow through a real nozzle because frictional losses associated with the boundary layer will reduce the actual flow velocity from the theoretical ideal. However, if the nozzle is smoothly rounded (not just an abrupt contraction as shown in Fig. 6-16) and the throat Reynolds number is in excess of 10^4, then Eqs. (7-4), (7-5), and (7-28) are often accurate to within 93 to 99%. Design data on frictional losses in real nozzle designs are presented in the following section.

7.3. NOZZLE DISCHARGE COEFFICIENT

Definition. The actual flow rate through a nozzle seldom, if ever, equals the theoretical flow rate. Dissipation due to viscous friction and blockage of flow area by the boundary layer tend to reduce the flow rate below the theoretical ideal. A discharge coefficient, denoted by the symbol C, is introduced to correct the isentropic, one-dimensional theoretical flow rate:

$$C = \frac{\text{Actual Mass Rate of Flow}}{\text{Theoretical Mass Rate of Flow}}. \tag{7-31}$$

The mass flow through a nozzle with a discharge coefficient of C = 1 conforms exactly to the theoretical model.

The discharge coefficient is generally a function of the nozzle geometry, Reynolds number, and, for compressible flow, Mach number:

$$C = F(\text{nozzle geometry}, UD/\nu, U/c). \tag{7-32}$$

U is typically the inlet velocity, D is the inlet diameter, and c is the speed of sound. Values of the discharge coefficient for a number of nozzles are given in Table 7-5.

Using Eq. (7-5), the mass flow through an incompressible fluid through a nozzle is expressed in terms of the static pressures p_1 and p_2 associated with the flow areas A_1 and A_2 and the discharge coefficient C,

$$\dot{m} = C\rho U_2 A_2 = CA_2 \left[\frac{1}{1 - (A_2/A_1)^2} \right]^{1/2} [2\rho(p_1 - p_2)]^{1/2} \tag{7-33}$$

5

Table 7-3. Expansion Coefficients for Nozzles.

Notation: d = nozzle throat diameter; D = pipe diameter; p_1 = static pressure upstream of nozzle; p_2 = static pressure at nozzle throat; γ = ratio of specific heat at constant pressure to that at constant volume. [Eq. (7-29); Ref. 7-10, p. 224.]

	Expansion Factor Y for γ = 1.3								
	Pressure Ratio, p_2/p_1								
d/D	.095	0.90	0.85	0.80	0.75	0.70	0.65	0.60	0.55
0.2	0.9707	0.9407	0.9099	0.8781	0.8454	0.8117	0.7768	0.7406	0.7030
.3	.9705	.9402	.9092	.8773	.8445	.8106	.7756	.7393	.7016
.4	.9698	.9390	.9074	.8750	.8417	.8075	.7722	.7357	.6978
0.50	.9683	.9362	.9034	.8700	.8358	.8008	.7648	.7278	.6896
.55	.9671	.9338	.9001	.8658	.8309	.7952	.7588	.7214	.6829
.60	.9654	.9305	.8954	.8599	.8240	.7876	.7505	.7126	.6738
0.65	.9629	.9259	.8889	.8519	.8146	.7771	.7392	.7007	.6614
.70	.9594	.9193	.8798	.8406	.8016	.7627	.7237	.6844	.6447
.725	.9570	.9150	.8739	.8333	.7933	.7535	.7139	.6742	.6343
0.75	.9542	.9098	.8667	.8246	.7833	.7426	.7023	.6622	.6221
.775	.9507	.9034	.8580	.8141	.7714	.7297	.6886	.6481	.6077
.80	.9462	.8955	.8473	.8013	.7570	.7141	.6723	.6313	.5908
0.82	.9418	.8876	.8368	.7888	.7431	.6992	.6568	.6155	.5750
.84	.9362	.8779	.8241	.7739	.7266	.6817	.6387	.5971	.5567
.86	.9292	.8658	.8084	.7557	.7067	.6608	.6172	.5756	.5353

	Expansion Factor Y for γ = 1.4								
	Pressure Ratio, p_2/p_1								
d/D	0.95	0.90	0.85	0.80	0.75	0.70	0.65	0.60	0.55
0.2	0.9728	0.9448	0.9160	0.8863	0.8556	0.8238	0.7908	0.7565	0.7207
.3	.9726	.9444	.9154	.8855	.8546	.8227	.7896	.7552	.7193
.4	.9719	.9432	.9137	.8833	.8520	.8198	.7864	.7517	.7156
0.50	.9706	.9405	.9099	.8785	.8464	.8133	.7793	.7441	.7076
.55	.9694	.9383	.9067	.8745	.8416	.8080	.7734	.7378	.7010
.60	.9678	.9352	.9023	.8690	.8351	.8006	.7653	.7292	.6920
0.65	.9655	.9309	.8962	.8613	.8261	.7905	.7543	.7175	.6798
.70	.9622	.9247	.8876	.8506	.8136	.7765	.7392	.7016	.6633
.725	.9600	.9207	.8819	.8436	.8056	.7676	.7297	.6915	.6530
0.75	.9573	.9158	.8751	.8353	.7960	.7571	.7184	.6797	.6409
.775	.9540	.9097	.8669	.8252	.7845	.7445	.7050	.6657	.6266
.80	.9498	.9022	.8566	.8128	.7705	.7292	.6889	.6491	.6097
0.82	.9457	.8947	.8466	.8009	.7570	.7147	.6736	.6334	.5939
.84	.9405	.8856	.8344	.7864	.7409	.6975	.6557	.6152	.5755
.86	.9338	.8740	.8194	.7688	.7215	.6769	.6344	.5936	.5541

Original Edition 1984
Reprint Edition 1992 w/corrections

Printed and Published by
KRIEGER PUBLISHING COMPANY
KRIEGER DRIVE
MALABAR, FLORIDA 32950

Copyright © 1984 by Van Nostrand Reinhold Company, Inc.
Reprinted by Arrangement.

All rights reserved. No part of this book may be reproduced in any form or by any means, electronic or mechanical, including information storage and retrieval systems without permission in writing from the publisher.
No liability is assumed with respect to the use of the information contained herein.
Printed in the United States of America.

FROM A DECLARATION OF PRINCIPLES JOINTLY ADOPTED BY A COMMITTEE OF THE AMERICAN BAR ASSOCIATION AND COMMITTEE OF PUBLISHERS:

This Publication is designed to provide accurate and authoritative information in regard to the subject matter covered. It is sold with the understanding that the publisher is not engaged in rendering legal, accounting, or other professional service. If legal advice or other expert assistance is required, the services of a competent professional person should be sought.

Library of Congress Cataloging-Publication Data

Blevins, Robert D.
Applied fluid dynamics handbook / Robert D. Blevins. — Reprint ed. w. corrections.
p. cm.
Originally published: New York, N. Y. : Van Nostrand Reinhold Co., c1984.
Includes bibliographical references and index.
ISBN 0-89464-717-2
1. Fluid dynamics—Handbooks, manuals, etc. I. Title.
TA357.B57 1992
620. 1 ' 06—dc20 92-4247
CIP

10 9 8 7 6 5 4 3 2

7

THERMOPHYSICAL PROPERTIES OF HELIUM

PRESSURE = 0.120 [MPa]

	TEMP [K]	DENSITY [kg/m³]	PV/RT [-]	ENERGY [J/g]	ENTHALPY [J/g]	ENTROPY [J/g·K]	C_V [J/g·K]	C_P [J/g·K]	VSOUND [m/s]
	0.8000	147.2	0.4905	0.7170E-02	0.8223	0.4265E-02	0.2231E-01	0.2233E-01	248.4
	1.000	147.2	0.3924	0.1804E-01	0.8332	0.1614E-01	0.1027	0.1027	246.4
	1.200	147.2	0.3270	0.5750E-01	0.8728	0.5150E-01	0.3233	0.3233	246.8
	1.400	147.2	0.2802	0.1839	0.9789	0.1324	0.7864	0.7888	246.9
	1.600	147.3	0.2450	0.3879	1.212	0.2871	1.813	1.817	245.7
	1.800	147.5	0.2175	0.6484	1.680	0.5491	2.957	2.984	242.0
	2.000	147.9	0.1954	1.847	2.458	0.9877	5.238	5.263	235.4
1	2.088	148.0	0.1839	2.035	2.848	1.158	8.487	8.529	232.8
2	2.158	148.4	0.1836	2.758	3.587	1.499	10.43	10.59	228.8
3	2.185	148.4	0.1798	2.883	3.871	1.548	13.18	13.54	228.1
3	2.167	148.4	0.1796	2.887	3.889	1.559	8.070	8.120	228.8
2	2.178	148.4	0.1788	2.942	3.750	1.584	5.083	5.083	229.5
1	2.288	148.3	0.1718	3.247	4.058	1.722	2.888	2.734	231.3
	2.400	147.8	0.1828	3.571	4.383	1.882	2.157	2.294	232.5
	2.700	148.1	0.1484	4.218	5.039	2.120	1.984	2.240	230.3
	3.000	143.6	0.1338	4.902	5.738	2.384	2.008	2.472	226.2
	3.300	140.9	0.1243	5.669	6.541	2.620	2.188	2.910	219.3
	3.600	137.2	0.1170	6.614	7.488	2.894	2.344	3.413	208.9
	3.900	132.6	0.1117	7.695	8.600	3.190	2.456	4.035	196.1
	4.200	126.6	0.1068	8.988	9.933	3.518	2.538	4.950	182.8
L	4.407	121.1	0.1083	10.08	11.07	3.782	2.585	6.137	186.8
V	4.407	20.17	0.6499	24.69	30.61	8.208	3.198	10.34	100.3
	4.500	18.98	0.6772	25.20	31.53	8.414	3.193	8.407	103.5
	4.800	18.24	0.7412	26.70	34.09	8.985	3.171	7.687	112.0
	5.000	14.97	0.7721	27.59	35.81	9.278	3.157	7.381	118.8
	5.100	14.43	0.7852	28.01	36.33	9.420	3.150	7.185	119.0
	5.300	13.49	0.8081	28.84	37.73	9.689	3.140	6.858	123.1
	5.500	12.70	0.8273	29.63	38.08	9.839	3.131	6.628	127.0
	6.000	11.14	0.8644	31.52	42.29	10.50	3.117	6.245	135.7
	6.500	9.876	0.8908	33.32	45.35	10.99	3.111	6.012	143.4
	7.000	9.082 9.604	0.9107	35.07	48.32	11.43	3.108	5.858	150.4
	8.000	7.699	0.9360	38.48	54.07	12.19	3.109	5.663	163.1
	9.000	6.718	0.9555	41.80	58.67	12.85	3.112	5.549	174.4
	10.00	5.972	0.9874	45.06	65.18	13.44	3.114	5.475	184.9
	12.00	4.903	0.9819	51.55	78.03	14.42	3.118	5.385	203.7
	15.00	3.660	0.9925	61.14	92.07	15.62	3.121	5.315	228.7
	20.00	2.690	0.9995	78.97	118.5	17.14	3.122	5.281	264.5
	25.00	2.306	1.002	92.70	144.7	18.31	3.121	5.236	283.7
	30.00	1.920	1.003	109.4	170.9	19.26	3.121	5.222	323.8
	40.00	1.440	1.003	139.7	223.0	20.76	3.118	5.209	373.7
	50.00	1.152	1.003	170.9	275.1	21.92	3.119	5.202	417.5
	60.00	0.9603	1.003	202.1	327.1	22.87	3.118	5.159	457.1
	80.00	0.7208	1.002	264.5	431.0	24.37	3.117	5.155	527.4
	100.0	0.5767	1.002	328.6	534.9	25.53	3.117	5.195	589.4
	120.0	0.4807	1.001	399.2	639.8	26.47	3.117	5.194	645.5
	140.0	0.4121	1.001	451.5	742.7	27.26	3.117	5.194	697.0
	160.0	0.3607	1.001	513.6	846.6	27.97	3.116	5.193	745.0
	180.0	0.3208	1.001	576.2	950.4	28.58	3.116	5.193	790.1
	200.0	0.2886	1.001	638.5	1054.	29.13	3.116	5.193	832.1
	220.0	0.2624	1.001	700.8	1158.	29.62	3.118	5.193	873.1
	240.0	0.2405	1.001	763.1	1262.	30.07	3.118	5.193	912.
	260.0	0.2220	1.001	825.4	1366.	30.49	3.116	5.193	949.
	280.0	0.2062	1.001	887.6	1470.	30.87	3.116	5.193	985.
	300.0	0.1925	1.001	950.1	1574.	31.23	3.116	5.193	1020
	350.0	0.1650	1.000	1106.	1833.	32.03	3.116	5.193	1101
	400.0	0.1444	1.000	1262.	2083.	32.73	3.118	5.193	1177
	500.0	0.1155	1.000	1573.	2812.	33.69	3.116	5.193	1311
	600.0	0.9626E-01	1.000	1885.	3131.	34.83	3.116	5.193	144
	700.0	0.8251E-01	1.000	2186.	3851.	35.83	3.116	5.193	155
	800.0	0.7220E-01	1.000	2506.	4170.	36.33	3.118	5.193	166
	900.0	0.6416E-01	1.000	2820.	4888.	36.94	3.118	5.193	176
	1000.	0.5776E-01	1.000	3131.	5209.	37.49	3.116	5.193	186
	1100.	0.5251E-01	1.000	3443.	5726.	37.98	3.116	5.193	195
	1200.	0.4814E-01	1.000	3754.	6247.	38.43	3.118	5.193	205
	1300.	0.4443E-01	1.000	4066.	6767.	38.85	3.116	5.193	214
	1400.	0.4126E-01	1.000	4376.	7286.	39.23	3.116	5.193	223
	1500.	0.3851E-01	1.000	4689.	7805.	39.59	3.116	5.193	232

8